NJC

ROYAL SOCIETY OF CHEMISTRY

PAPER

View Article Online
View Journal | View Issue

Check for updates

Cite this: *New J. Chem.*, 2024, **48**, 8343

Photorelease of nitric oxide from Pluronic F127/chitosan hydrogels incorporating a water soluble ruthenium nitrosyl complex†

Hazem Gzam,[a] Dalel Katar,[a] Marine Tassé,[a] Yue Xiao,[a] Isabelle Malfant,*[a] Juliette Fitremann,[b] Patricia Vicendo,[b] Anne-Françoise Mingotaud*[b] and Dominique de Caro*[a]

Received 13th February 2024,
Accepted 20th March 2024

DOI: 10.1039/d4nj00724g

rsc.li/njc

In this paper, the NO donor *trans*-(Cl,Cl)-[Ru(FT)Cl_2(NO)]Cl (Ru–NO) was incorporated in a Pluronic F127 (PL)–chitosan (CS) biocompatible hydrogel. Two concentrations were achieved (520 and 13 μg g^{-1}), resulting in hydrogels with sol–gel transition temperatures of around 36–38 °C, according to rheological studies. The presence of the Ru–NO complex did not significantly modify the thermal (DSC) and morphological (AFM) characteristics of the gels. For Ru–NO-embedded hydrogels, nitric oxide photorelease was evidenced at 400 nm. The quantum yield of photorelease was independent of the temperature at which the gel was maintained (25, 31, or 37 °C) and was found to be *ca.* 0.015. EPR as well as measurements using an electrochemical NO sensor also confirmed NO release upon light irradiation at 400 nm.

Open Access Article. Published on 05 April 2024. Downloaded on 6/6/2026 6:34:21 AM.
This article is licensed under a Creative Commons Attribution-NonCommercial 3.0 Unported Licence.

1. Introduction

Although nitric oxide is generally considered to be a polluting and toxic gas, its role in various physiological processes explains the interest shown in recent years in NO-donating compounds, particularly metal nitrosyl complexes.[1] Among them, ruthenium nitrosyl complexes are of great interest because they generate NO rapidly at the biological target site under light stimuli.[2] Furthermore, in order to prepare an applicable system, the encapsulation of ruthenium nitrosyl complexes in polymers has been investigated by several research groups. E. Tfouni *et al.* reported on the encapsulation of *trans*-[Ru(NO)$(NH_3)_4$(py)]$(BF_4)_3$·H_2O (py = pyridine) in poly-lactic-*co*-glycolic acid microparticles,[3] whereas A. Schiller *et al.* described the embedding of a ruthenium nitrosyl complex containing a bisimidazole biscarboxamide ligand into nanofibrous non-woven poly(L-lactide-*co*-D/L-lactide).[4] A. S. Borovik *et al.* have reported on the synthesis of a highly cross-linked, porous polymer network containing immobilized Ru–NO sites.[5] D. W. Franco *et al.* also described the impregnation of the *trans*-[Ru$(NH_3)_4$(isn)(NO)]$(BF_4)_3$ (isn = isonicotinamide) into cassava starch.[6] The resulting biodegradable films were shown to release NO either by light irradiation (355 nm) or by chemical reduction using L-cysteine as a reducing agent. Finally, E. Tfouni *et al.* reported the immobilization of the $[Ru(NH_3)_4(NO)]^{3+}$ ion on modified silica gel surfaces.[7,8] The hybrid materials thus obtained evidenced NO release by chemical reduction with Eu(II) ions. Regeneration of the immobilized Ru–NO complex was achieved by reaction with NO_2^- ions in aqueous solution.

Hydrogels can be viewed as three-dimensional hydrophilic polymeric networks able to absorb a high-water content exhibiting soft consistency. Examples of hydrogels incorporating a nitro- or a nitroso-ruthenium complex are very rare. R. F. V. Lopez *et al.* described the preparation of hydroxyethyl cellulose, polyacrylate or chitosan-based hydrogels saturated with *cis*-$[Ru(NO_2)(bipyridine)_2(4\text{-picoline})]^+$.[9] The NO release was evidenced after irradiation using a Hg-lamp light. On the other hand, P. K. Mascharak *et al.* reported on the covalent attachment of a ruthenium nitrosyl complex bearing the 4-vinylpyridine ligand on a poly(2-hydroxyethyl methacrylate)/ethyleneglycol dimethacrylate (pHEMA) hydrogel.[10] Further exposure to UV-light (360 nm) promoted photorelease of NO. Finally, J. G. Liu *et al.* described the dispersion of Fe_3O_4@polydopamine@Ru–NO@folic acid nanoplatforms into a poly(vinyl alcohol)/chitosan-based hydrogel.[11] The NO release was performed in the near infrared region, *i.e.*, 808 nm. The nitric oxide photorelease can be achieved in the visible range for ruthenium nitrosyl complexes bearing the FT ligand (FT = 4′-(9*H*-fluoren-2-yl)-2,2′:6′,2″-terpyridine), such as *cis*-(Cl,Cl)- and *trans*-(Cl,Cl)-[Ru(FT)Cl_2(NO)][X) (X = Cl or PF_6).[12,13]

[a] *Laboratoire de Chimie de Coordination du CNRS, 205 route de Narbonne, F-31077 Toulouse, France. E-mail: dominique.decaro@lcc-toulouse.fr*
[b] *Softmat, Université de Toulouse, CNRS UMR 5623, Université de Toulouse III - Paul Sabatier, 118 route de Narbonne, 31062 Toulouse cedex 9, France*

† Electronic supplementary information (ESI) available: Infrared spectra and complementary rheological data for hydrogels. See DOI: https://doi.org/10.1039/d4nj00724g

Open Access Article. Published on 05 April 2024. Downloaded on 6/6/2026 6:34:21 AM.
This article is licensed under a Creative Commons Attribution-NonCommercial 3.0 Unported Licence.

The *trans*-(Cl,Cl)-[Ru(FT)Cl_2(NO)](PF_6) isomer has also been recently used to grow the first ruthenium nitrosyl-based nanoparticles.[14]

Pluronic F127 (PL) is known to spontaneously self-organize in aqueous media due to the solubility difference between poly(ethylene oxide) and poly(propylene oxide) units, leading to the formation of micelles.[15] These micelles auto-assemble when the temperature increases, leading to a 3-D polymeric network. Pluronic F127-based hydrogels are known to incorporate organic NO donors leading to biocompatible and antibacterial materials.[16,17] Chitosan (CS), a biocompatible and non-allergenic polysaccharide exhibiting good muco-adhesive properties, associated with PL leads to thermoresponsive PL/CS hydrogels. These latter have been used to incorporate the NO donor *S*-nitrosoglutathione (GSNO).[16] The NO release from GSNO was monitored at room, skin and physiological temperatures. The GSNO/PL/CS hydrogels exhibited antimicrobial activity to *Pseudomonas aeruginosa*. To our knowledge, PL/CS hydrogels incorporating a ruthenium nitrosyl complex have never been described. Here, we report on the synthesis, characterization and NO photorelease of PL/CS hydrogels containing a Ru–NO complex bearing the FT ligand.

2. Experimental

Pluronic F127 (MW = 12 600 g mol^{-1}, Fig. 1), chitosan (low molecular weight: 50 000–190 000 g mol^{-1}, Fig. 1), lactic acid and Griess reagent were commercially available (Sigma-Aldrich). Hydrogel syntheses were carried out using fresh distilled water (GFL Water Still 2004, conductivity: 1400 μS cm^{-1} at 25 °C). *Trans*-(Cl,Cl)-[dichlorido(4′-(9*H*-fluoren-2-yl)-2,2′:6′,2″-terpyridine)nitrosylruthenium(II)]chloride (abbreviated as *trans*-(Cl,Cl)-[Ru(FT)Cl_2-(NO)]Cl, Fig. 1) was prepared according to a previous work.[13]

Synthesis of PL/CS hydrogels

PL/CS hydrogels were obtained in accordance with a previously published procedure.[16] 50 mg of CS, 100 mg of lactic acid and 5 mL of water were added into a 25 mL beaker. The mixture was stirred (600 rpm) at room temperature for 15 min until a viscous liquid was obtained. The beaker was then placed at 4 °C and 1 g of PL was progressively and slowly added under stirring (280 rpm) until the polymer was completely dissolved (~45 min). The hydrogel thus obtained (abbreviated as HB, B for the blank) was then stored at 4 °C in a capped flask.

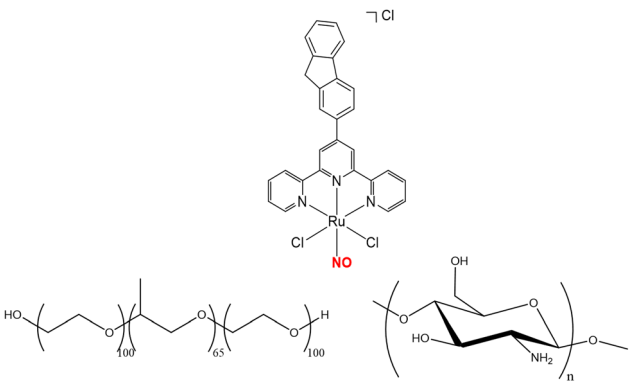

Fig. 1 Molecular formula for *trans*-(Cl,Cl)-[Ru(FT)Cl_2(NO)]Cl (top), Pluronic F127 (bottom left) and chitosan (bottom right).

Synthesis of PL/CS hydrogels incorporating a Ru–NO complex

The *trans*-(Cl,Cl)-[Ru(FT)Cl_2(NO)]Cl stock solution (1 mM) was obtained by dissolving 3.2 mg of the complex in 5 mL of water for 20 min under ultrasound. As already described,[13] the complete transformation of the *trans*-(Cl,Cl)-[Ru(FT)Cl_2(NO)]$^+$ ion into the *trans*-(NO,OH)-[chlorido(4′-(9*H*-fluoren-2-yl)-2,2′:6′,2″-terpyridine)hydroxonitrosylruthenium(II)] ion (abbreviated as *trans*-(NO,OH)-[Ru(FT)Cl(NO)(OH)]$^+$) for 48 h at 25 °C was monitored by UV-vis spectroscopy using a Cary 60 UV-Visible spectrophotometer.

Two hydrogels were prepared as follows:

(i) 50 mg of CS, 100 mg of lactic acid and the complex whole complex stock solution were added into a 25 mL beaker. The rest of the synthetic procedure was identical to that described for HB. This Ru–NO/PL/CS hydrogel (stored at 4 °C in a capped flask) was abbreviated as HC1 (C for the complex).

(ii) 50 mg of CS, 100 mg of lactic acid, 5 mL of water and 125 μL of the complex stock solution were added into a 25 mL beaker. The rest of the synthetic procedure was identical to that described for HB. This Ru–NO/PL/CS (stored at 4 °C in a capped flask) was abbreviated as HC2.

Characterization

Infrared spectra were recorded at 25 °C on a ground sample of the dried hydrogel on a PerkinElmer Spectrum 100 FT-IR spectrometer using a diamond ATR (GladiATR from PIKE technologies). ^{1}H NMR spectra were recorded on a Bruker Avance 400 spectrometer at 25 °C using deuterated DMSO. Electrospray ionization mass spectra were acquired using a Thermo Scientific LCQ Fleet spectrometer.

Thermogravimetric measurements were carried out on a sample of the hydrogel (15 μL) placed in an aluminum pan, using a METTLER TOLEDO TGA/DSC 3+ thermal analysis system. Samples were heated from 25 to 600 °C under nitrogen. Thermal characterization by differential scanning calorimetry (DSC) was performed using a NETZSCH DSC 3500 SIRIUS equipment. The reference was an aluminum sample holder. Hydrogels (10 mg placed in a sealed aluminum sample holder) were studied using the following thermal cycle: 21 to −65 °C at 10 °C min^{-1} and heating from −65 to 60 °C at 10 °C min^{-1}.

Atomic force microscopy was performed using a Smart SPM-100 AIST-NT microscope. (001)-oriented Si substrates (1 cm^2) were previously cleaned with acetone, ethanol and distilled water, and finally dried under a nitrogen flow. A drop of hydrogel (50 μL) was deposited on the substrate, spread out with a glass slide and gently dried at 25 °C for 50 min in the absence of dust. Images were acquired in tapping mode (resonance frequency: 325 kHz) with a silicon tip MikroMasch HQ-NSC15/AIBS.

 This journal is © The Royal Society of Chemistry and the Centre National de la Recherche Scientifique 2024

Open Access Article. Published on 05 April 2024. Downloaded on 6/6/2026 6:34:21 AM. This article is licensed under a Creative Commons Attribution-NonCommercial 3.0 Unported Licence.

Photokinetic studies on the photolysis reactions were carried out with a Cary 60 UV-Visible spectrophotometer equipped with a cooling water regulator. The temperature was maintained at 25, 31 or 37 °C during the experiments. Irradiation was performed from a chassis wheeled wavelength-switchable LED source from Mightex Company operating at 400 nm. Hydrogel samples (2 mL) were placed in a quartz cuvette of 1 cm path-length and the optical fiber was fixed laterally from it (distance source-cuvette: 5 mm). The light power (6 mW) was measured with a power meter from Thorlabs. Absorption spectra were taken after each 10 s for 25 min.

The light intensity (I_0) was determined before the photolysis experiments. The quantum yield (ϕ_{NO}) was determined using the program Sa3.3 written by D. Lavabre and V. Pimienta.[18] This allowed the resolution of differential eqn (1) from the model A → B:

$$\frac{d[A]}{dt} = -\phi_{NO} I_a^A = -\phi_{NO} Abs_A^{\lambda} I_0 F \quad (1)$$

where I_a^A is the intensity of the light absorbed by the precursor *A*, Abs_A^{λ} is the absorbance before irradiation, I_0 is the incident intensity measured at 400 nm, and *F* is the photokinetic factor given by eqn (2):

$$F = \frac{1 - Abs_{Tot}^{\lambda}}{Abs_{Tot}^{\lambda}} \quad (2)$$

where Abs_{Tot}^{λ} is the total absorbance. The equation was fitted with the experimental data $Abs_{Tot}^{\lambda} = f(t)$ and two parameters ϕ_{NO} and ε_B (ε_B is the molar extinction coefficient measured at the end of the reaction) at two wavelengths (irradiation at λ_{irr} = 400 nm and observation at λ_{obs} = 330 nm). The observation wavelength λ_{obs} was chosen because it corresponds to a large difference between the molar extinction coefficient at the initial and final times of the photochemical reaction. Simulation and optimization procedures were performed by using numerical integration and a non-linear minimization algorithm for the fitting of the model to the experimental data.[18,19]

Electron paramagnetic resonance (EPR) spectra were collected using a Bruker ESP 500E (X band) spectrometer. Previously synthetized *N*-methyl-D-glucamine dithiocarbamate (3.1 mg, 10^{-5} mol) reacted with Mohr's salt (125 μL of a 20 mM aqueous solution) to obtain $Fe(MGD)_2$. 90 μL of the hydrogel and 10 μL of the $Fe(MGD)_2$ solution were mixed and injected into a quartz capillary. Samples were irradiated at 400 nm for 6 min at 25 °C, the lamp being in contact with the EPR tube (power of the light source: 26 mW).

The quantitative determination of NO production was performed with a commercial NO detector (ami-NO 700) from Innovative Instruments Inc. The calibration of the electrode in the range of 50–1000 nM was performed by generating NO according to the following reaction:

$$2NO_2^- + 4H^+ + 2I^- \rightarrow 2NO^{\bullet} + I_2 + 2H_2O$$

For each calibration, aliquots (80 μL) of aqueous $NaNO_2$ (~100 μM) were added to 20 mL of a 0.03 M KI solution in 0.1 M H_2SO_4. Chronoamperograms were recorded at a fixed temperature (25 °C) while stirring the solution in order to maintain a constant rate of oxidation of the produced NO at the electrode surface. The typical sensitivity of the electrode was about 20 pA nM^{-1}. During photolysis measurements, the NO sensor was positioned outside the light path. Besides, chronoamperograms of distilled water were systematically recorded upon irradiation in order to subtract the light interference. Then, chronoamperograms were recorded upon irradiation at 400 nm of 2.5 mL of the hydrogel for 320 s at 25 °C (power of the light source: 26 mW).

Griess test

The Griess reagent (10 g) was dissolved in 250 mL of distilled water. A Ru–NO/PL/CS hydrogel was prepared following the procedure (ii) described above in the presence of 3 mL of the Griess reagent solution and 2 mL of distilled water to maintain a constant total volume of 5 mL. The hydrogel was then irradiated at 400 nm (power: 6 mW, distance source-cuvette: 5 mm). UV-vis spectra (Cary 60 UV-Visible spectrophotometer) were recorded every 12 s (at 25 °C) and the absorbance at 508 nm owing to the formation of the pink azo dye was measured to evidence the formation of the NO species.

Stability of hydrogels placed under saline aqueous conditions

1.5 mL of hydrogel (HB or HC1) at 4 °C (sol state) was added into a 15 mL-flask (hydrogel top surface: 3.1 cm^2), heated up to the physiological temperature (37 °C, gel state) and the flask was weighed. 3 mL of phosphate buffered saline (PBS) at 37 °C was gently added and the flask was weighed. The flask was then maintained at 37 °C for 1 h. The liquid phase and the hydrogel in the gel state were separated. The liquid phase was finally weighed to evaluate the mass of the hydrogel released in the saline solution.

Ru–NO release into phosphate buffered saline

The liquid phase separated from the hydrogel in the gel state (see above) was studied by UV-vis spectroscopy after 1 hour. The absorbance of the band at 403 nm was used to determine the percentage of Ru–NO released from the hydrogel.

Rheological measurements

The rheological properties of the hydrogels have been measured with a rheometer MCR301 Anton Paar equipped with a Peltier device for temperature control and a regulation bath for the Peltier set at 20 °C. The geometry was a transparent plate (glass) as the lower plate and a sandblasted stain less steel plate (diameter: 25 mm) as the upper plate. The gap was set at 500 μm. A cover was adjusted around the geometry to limit evaporation during the measurement. Below the transparent plate was placed an optical fiber (liquid light guide) linked to a Mightech multiple LED source that can illuminate the whole surface of the sample. This set up has been used whatever the experiment, with or without irradiation. In the case of experiments carried out with irradiation, the light was emitted by a monochromatic LED at 415 nm, 1000 mA. The light power was measured with a

Open Access Article. Published on 05 April 2024. Downloaded on 6/6/2026 6:34:21 AM.
This article is licensed under a Creative Commons Attribution-NonCommercial 3.0 Unported Licence.

photometer Maestro (Gentec-eo), by placing the detector in contact with the glass lower plate, with the cover around the geometry. The light power measured was 20 ± 5 mW cm^{-2}. The lamp was turned on manually at launching the rheological measurement.

Different oscillatory experiments have been performed with the following settings. The elastic and the viscous moduli have been recorded under these different conditions. Frequency sweep: the frequency was varied from 10 to 0.1 Hz at a fixed temperature (37 °C) and a shear strain (0.2%). Determination of the linear viscoelastic region: the shear strain was varied from 0.1 to 1000% at 37 °C and at 1 Hz in frequency. Temperature sweep: the shear strain and the frequency were fixed (resp. 0.2%/1 Hz) and the temperature was varied from 4 °C to 54 °C at 2 °C min^{-1}. Time sweep: G' and G'' were monitored with time, with data acquisition every 0.2 min, frequency at 1 Hz, shear strain at 0.2% and temperature set at the required value (20 °C or 37 °C). A typical sequence for the characterization of the viscoelastic properties of one sample was the temperature increase from 4 to 54 °C, 1 Hz, 0.2%; temperature stabilization step for 10 minutes at 20 °C to switch back to the liquid state; temperature stabilization step for 10 min at 37 °C to switch back to the gel state; frequency sweep at 37 °C, 0.2%; and shear strain sweep at 37 °C, 1 Hz. A typical sequence for characterizing the effect of irradiation on the gels was after loading, the sample was stabilized at 20 °C for 5 min, then at 37 °C for 5 min, and then the irradiation was powered on and at the same time a time sweep was launched on the sample, by measuring G' and G'' for 10 min with a frequency at 1 Hz, a strain at 0.2%, 37 °C. The time of gelation has also been tested by switching instantaneously the temperature from 20 °C to 37 °C and by monitoring G' and G'' for 10 min.

Before the measurement, samples were prepared as described above for HB, HC1 or HC2 and kept at 4 °C. The temperature of the rheometer plate was set at 4 °C, and then 320 µL of sample was transferred with an automatic pipette equipped with a truncated cone. Then, the gap and the cover were adjusted and the measurement was performed.

3. Results and discussion

Over the last few years, we have acquired extensive experience in the synthesis of ruthenium nitrosyl complexes bearing substituted terpyridine ligands. Most of them were not soluble in aqueous solution. However, the *trans*-(NO,OH)-[Ru(FT)Cl(NO)(OH)](PF$_6$) complex can be solubilized in water in the presence of 0.5% dimethyl sulfoxide.[20] This latter, in combination with methicillin and irradiated with a Hg lamp, was shown to decrease bacterial resistance and to make *Staphylococcus epidermidis* bacteria 100-fold less resistant to methicillin.[20] In the present work and in order to work in the sole presence of water as a solvent, we have selected the water-soluble *trans*-(Cl,Cl)-[Ru(FT)Cl$_2$(NO)]Cl complex. In water, a chlorido to hydroxo exchange was evidenced, leading to the *trans*-(NO,OH)-[Ru(FT)(Cl)(OH)(NO)]$^+$ cation.[13] As mentioned in the Introduction section, PL/CS hydrogels were used to physically absorb organic nitric oxide delivery systems. In the case of *S*-nitrosoglutathione, the PL/CS hydrogel acted as an excellent protector of the drug at a concentration of 50 mM.[16] However, the incorporation into a PL/CS hydrogel (containing ~80% of water), without demixing, of a molecule containing a metal centre is a challenge that seems a little more difficult to meet. The solubility limit of the *trans*-(Cl,Cl)-[Ru(FT)Cl$_2$(NO)]Cl complex was 3.2 mg in 5 mL of water (1 mM). Its complete transformation into the *trans*-(NO,OH)-[Ru(FT)Cl(NO)(OH)]Cl complex (now labelled as Ru–NO) was evidenced by UV-vis spectroscopy after two days at room temperature.[13] This solution, mixed with CS (0.8 wt%) and PL (16.3 wt%), led to an homogeneous yellow hydrogel (HC1). It was stored at 4 °C in the dark to avoid any NO release (520 µg g^{-1} of Ru–NO in the hydrogel matrix). A second hydrogel was prepared using a 25 µM Ru–NO solution in water, a concentration more in line with potential therapeutic applications. In this case and again in the presence of PL (16.3 wt%) and CS (0.8 wt%), an homogeneous pale yellow hydrogel (HC2) was elaborated and stored at 4 °C in the dark (13 µg g^{-1} of Ru–NO in the hydrogel matrix).

The morphologies of hydrogels (HB, HC1 and HC2) were investigated using atomic force microscopy on dried samples (Fig. 2). 20 µm × 20 µm images for the three hydrogels evidenced very similar nanorough surfaces. This nanoroughness constitutes a positive point for the cutaneous application of the hydrogel after it has dried on the skin.[21] Zoomed-in (5 µm × 5 µm) image on a roughly spherical area showed a heterogeneous and irregular structure which could be explained by shrinkage stresses in the polymeric network during water loss. It should be noted that for GSNO/PL/CS hydrogels,[16] scanning electron micrographs of lyophilized samples showed a transition from a smooth (without GSNO) to a microrough and porous (with 50 mM GSNO incorporated) surface. In our case, the lack of difference in morphology with and without Ru–NO could be explained by its low concentration, *i.e.* at most 1 mM.

The infrared spectra of hydrogels (HB, HC1 and HC2) were almost identical (Fig. S1, ESI†). Due to the low amount of Ru–NO, the NO stretching mode located at ~1890 cm^{-1} was not observed in the IR spectra of HC1 and HC2. Infrared spectra

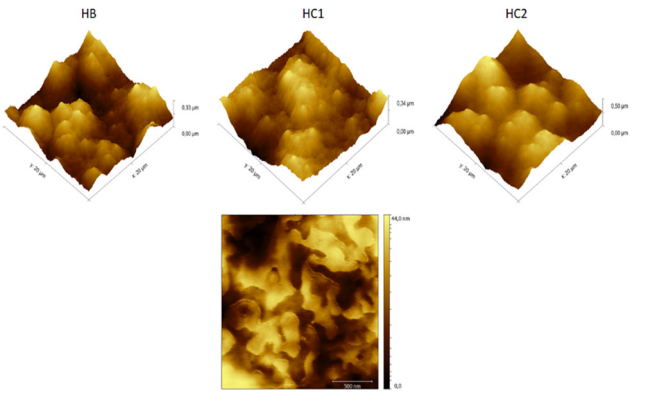

Fig. 2 AFM images of hydrogels (top: 3D views; down: top view of HB).

 This journal is © The Royal Society of Chemistry and the Centre National de la Recherche Scientifique 2024

Open Access Article. Published on 05 April 2024. Downloaded on 6/6/2026 6:34:21 AM.
This article is licensed under a Creative Commons Attribution-NonCommercial 3.0 Unported Licence.

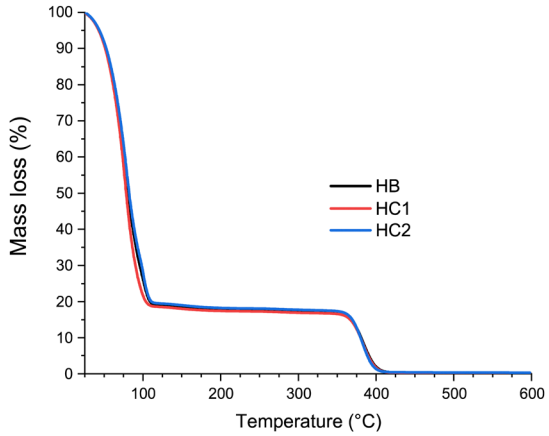

Fig. 3 Mass loss thermograms of hydrogels.

were dominated by those of PL, being the most present compound in the formulation. CH stretching modes were shown in the 2790–2880 cm^{-1} range whereas methylene scissor and wagging modes were located at 1466 and 1360 cm^{-1}, respectively. C–O–C modes at 1241 and 1279 cm^{-1} and C–O stretching mode at 1102 cm^{-1} were assigned according to previous studies.[21] The CO stretching mode at 1732 cm^{-1} was attributed to lactic acid. Finally, low intensity bands at 3400 (OH mode), 1653 (amide I band) and 1580 (amide II band) cm^{-1} confirmed the presence of CS in the gel.

The mass loss thermograms of HB, HC1 and HC2 showed an initial mass loss of 81% which ended at 110 °C and corresponded to the loss of all the water contained in the hydrogel (Fig. 3). The second mass loss of 29% (350–400 °C) was attributed to the decomposition of the organic matter. Differential scanning calorimetry thermograms of HB, HC1 and HC2 hydrogels were similar (Fig. 4). The sample, in its sol state, was initially cooled from 21 to −60 °C. An intense exothermic peak occurred between −18 and −21 °C, due to the crystallization of water contained in hydrogels. This phenomenon of delayed crystallisation was explained by the presence of water bound to the polymer network *via* hydrogen or van der Waals bonds.[22] As

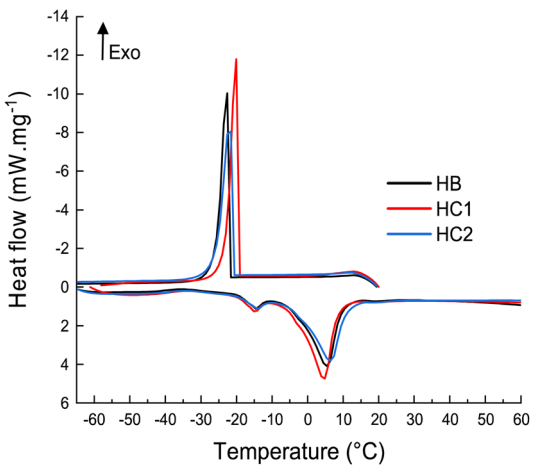

Fig. 4 DSC thermograms of hydrogels.

the sample warmed up, two endothermic signals were observed: a first low intensity peak at −15 °C and a second at ∼5–6 °C about 5–6 times more intense than the first. They were both assigned to the melting of water. The first peak (−15 °C) corresponded to the early melting of a certain amount of water (which had crystallised at a relatively close temperature, *i.e.* −18 °C), whereas the second was assigned to the late fusion of water (presumably due to the stabilisation of water crystals by PL chains).

The viscoelastic properties of the hydrogels loaded with Ru–NO or not loaded have been determined by rheology in oscillatory mode, by measuring the elastic modulus (G') and the viscous modulus (G'') as a function of different parameters. After determining the linear viscoelastic region (Fig. S2a and S3a, ESI†) and the response as a function of the frequency (Fig. S2b and S3b, ESI†), the sol–gel transition was determined by increasing the temperature, from 4 to 54 °C at 2 °C min^{-1}, for gels without Ru–NO (HB) and with Ru–NO (HC1) (Fig. 5). The transition temperature was taken as the temperature for which G' becomes higher than G''. This transition was slightly lower in the case of the HC1 gel (36 °C) than in the case of the HB gel (38 °C). The gelation time was also determined by switching instantaneously the temperature of the samples from 20 °C to 37 °C. The gelation was complete for HB (Fig. S2c, ESI†) and HC1 (Fig. S3c, ESI†) after 10 min (G' and G'' no longer varied). The G' values were of the order of 10 kPa for all the gels, which corresponded to very soft hydrogels. This value was not significantly different if the gel was loaded with Ru–NO or not loaded.

Ru–NO complexes bearing the FT ligand were known to release NO when irradiated in the UV, visible and near infrared regions of the electromagnetic spectrum.[12,13,23] The release of nitric oxide was followed by the formation of a photoproduct in which the NO ligand was substituted by a solvent ligand, according to the following equation:

$$(L)Ru^{II}(NO) + solvent \rightarrow (L)Ru^{III}(solvent) + NO^{\bullet}$$

UV-vis spectra recorded at 25 °C for the *trans*-(NO,OH)-[Ru(FT)Cl(NO)(OH)](PF$_6$) complex solubilized in water (0.5% DMSO) under irradiation at 420 nm showed the appearance of a band at 330 nm and the simultaneous disappearance of a band at 380 nm.[20] The presence of two isosbestic points at 346 and 426 nm indicated a clean conversion of the $Ru^{II}(NO^{+})$

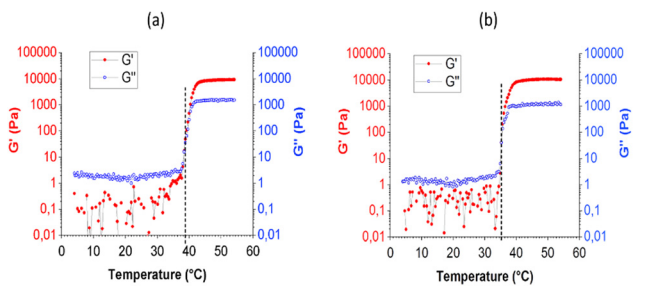

Fig. 5 Elastic (G') and viscous (G'') moduli as a function of temperature (2 °C min^{-1}): (a) HB and (b) HC1. The dotted line indicates the sol–gel temperature.

Open Access Article. Published on 05 April 2024. Downloaded on 6/6/2026 6:34:21 AM.
This article is licensed under a Creative Commons Attribution-NonCommercial 3.0 Unported Licence.

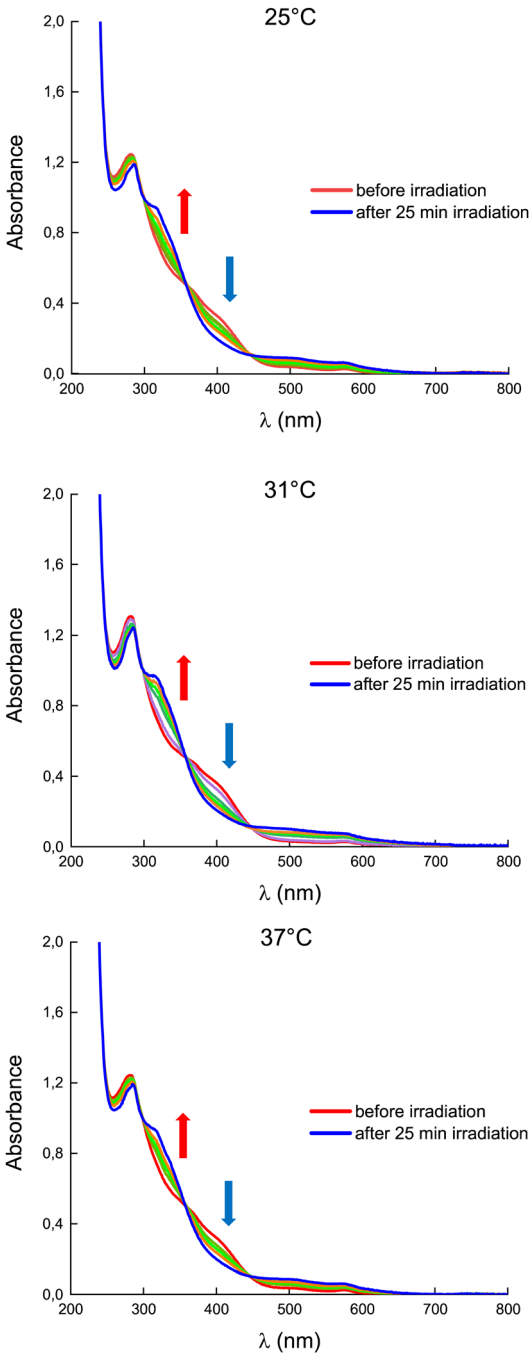

Fig. 6 Evolution in the absorption spectra of HC2 under irradiation at 400 nm.

complex into the photolysed species and no back-reaction was evidenced after turning off the incident light. The quantum yield of NO release was calculated at 0.020 (λ_{irr} = 420 nm). In our study, the photorelease study was performed at room (25 °C, sol state), skin (31 °C, sol state) and physiological (37 °C, gel state) temperatures on HC2 irradiated at 400 nm. For each temperature, the NO photorelease study was carried out three times and the results were very similar. Typical spectral evolutions are shown in Fig. 6.

Both in the sol and in the gel state, the presence of isosbestic points at 357 and 447 nm was in agreement with a clean conversion of the initial $Ru^{II}(NO)$ complex embedded in the hydrogel to the related photolysed complex. According to previous studies,[13] it can be assumed that the photolysed species formed in the hydrogel is a Ru^{III} complex in which a H_2O ligand entered the coordination sphere of the Ru centre instead of the NO ligand. Irradiated samples of $[Ru^{II}(FT)Cl_2(NO)]^+$ and $[Ru^{II}(FT)Cl(NO)(OH)]^+$ were known for not showing a X-band EPR signal.[12,13] This unexpected behaviour has occasionally been observed in Ru^{III} ions, which may be EPR silent due to fast electron spin relaxation, even at low temperatures.[24,25] However, the mass spectrum of HC2 irradiated at 400 nm for 25 min showed a signal at 569.04 uma, in excellent agreement with that for $[Ru^{III}(FT)Cl(H_2O)(OH)]^+$ (569.02 uma, Fig. S4, ESI†). This confirmed the replacement of the NO ligand by a H_2O ligand and the simultaneous change from oxidation state II to oxidation state III for Ru. Fig. 6 also evidences the appearance of a new band at 314 nm and the disappearance of the absorption at 403 nm. This latter was previously assigned to a transition involving the ruthenium-nitrosyl fragment.[12] Its disappearance upon irradiation was then consistent with the loss of the NO ligand. Spectra were also recorded in water at 25 °C for the *trans*-(NO,OH)-$[Ru(FT)Cl(NO)(OH)]^+$ cation under irradiation at 400 nm (in the absence of the hydrogel embedding the Ru–NO complex, Fig. S5, ESI†). They clearly evidenced the same shape as those for HC2 (Fig. 2). The two characteristic bands, which appear (334 nm) and disappear (402 nm) upon the photolysis process, were at similar positions to those for HC2 (314 and 403 nm, respectively). The model used to determine the NO photorelease quantum yield ϕ_{NO} assumed that the only absorbing species present were the initial complex and the photoproduct. Whatever the temperature (25, 31 or 37 °C) during the irradiation process (at 400 nm), quantum yields of about 0.015 were found. These values were of the same order of magnitude as that for the *trans*-(NO,OH)-$[Ru(FT)Cl(NO)(OH)](PF_6)$ complex solubilized in water/0.5% DMSO irradiated at 420 nm (0.020).[20] The Ru–NO complex, although embedded in the hydrogel, still showed good ability to release NO for an irradiation wavelength at the beginning of the visible range. However, our values were approximately twice as low as those for the *trans*-(NO,OH)-$[Ru(FT)Cl(NO)(OH)](PF_6)$ complex solubilized in water/0.5% DMSO[20] or dispersed as nanoparticles in water, both irradiated at 365 nm (~0.040).[14] The NO release upon irradiation at 400 nm of a hydrogel sample containing 25 μM of Ru–NO and the Griess reagent (0.04 g mL^{-1}) was verified by UV-vis spectroscopy at room temperature (Fig. 7). This test involved an oxidation of the NO photo-released to NO_2^- ions in aqueous solution followed by the reaction with sulfanilic acid leading to a diazonium cation. Its subsequent reaction with *N*-(1-naphthyl)ethylenediamine led to the formation of a pink azo dye. Fig. 7 clearly evidences the increase in the absorbance of the band located at 508 nm, confirming the gradual formation of the azo dye.

This experiment therefore undoubtedly proved that NO release took place under irradiation. It was important to note that the UV-vis spectrum did not show an absorption band in the 500–540 nm range when the HB hydrogel (containing no

 This journal is © The Royal Society of Chemistry and the Centre National de la Recherche Scientifique 2024

Open Access Article. Published on 05 April 2024. Downloaded on 6/6/2026 6:34:21 AM.
This article is licensed under a Creative Commons Attribution-NonCommercial 3.0 Unported Licence.

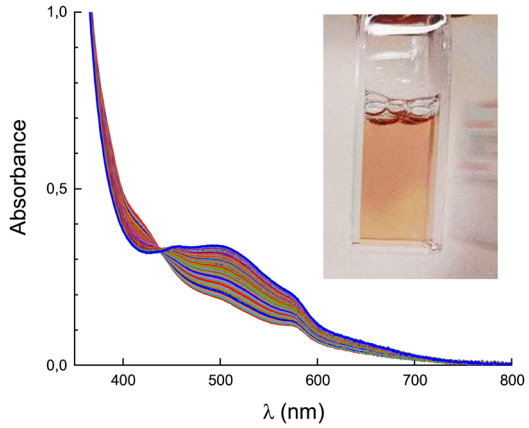

Fig. 7 Evolution in the absorption spectra of HC2 in the presence of the Griess reagent under irradiation at 400 nm at 25 °C. Inset: Picture of the cuvette after irradiation of the upper zone of HC2, showing the characteristic pink azo dye.

Ru–NO) was irradiated at 400 nm in the presence of the Griess reagent. Additional evidence of NO release could be provided by EPR or by using a NO• sensor. EPR spectroscopy allowed a direct observation of the NO• radical after the reaction with a spin trap leading to the [Fe^{II}–NO(MGD)$_2$] complex after photorelease induced by irradiation at 400 nm at 25 °C. The EPR spectrum of HC1 (520 μg g^{-1} of Ru–NO in the hydrogel matrix) showed a characteristic triplet signal with a hyperfine splitting constant value of a_N = 1.23 × 10^{-3} cm^{-1} and a *g*-factor of *g* = 2.127 (Fig. 8). No EPR signal was observed for HC2 (13 μg g^{-1} of Ru–NO in the hydrogel matrix) due to a lack of sensitivity of this technique for a very low Ru–NO content. For HC2, the NO• release was detected directly and quantitatively in the sol state (at 25 °C) by the use of the NO• sensor. The resulting chronoamperograms indicated a concentration of the NO• radical up to *ca.* 220 nM after an irradiation of *ca.* 300 s at 400 nm (Fig. 9). P. K. Mascharak *et al.* also evidenced the NO• release from a ruthenium nitrosyl complex covalently bonded to a pHEMA hydrogel, using an electrochemical nitric oxide sensor (λ_{irr} = 350 nm).[10] In our case, all three techniques (Griess test, EPR, and NO• sensors) were used to evidence the NO photorelease at

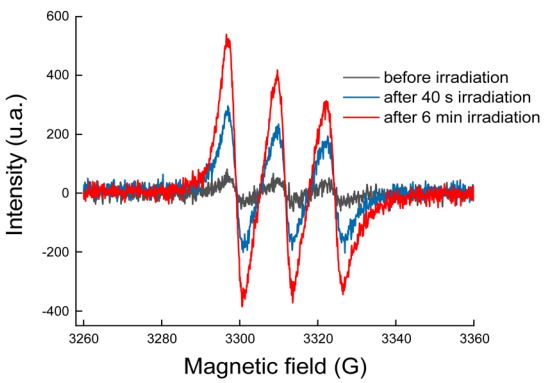

Fig. 8 EPR signals for the [FeII-NO(MGD)$_2$] adduct upon irradiation at 400 nm (sample: HC1 at 25 °C).

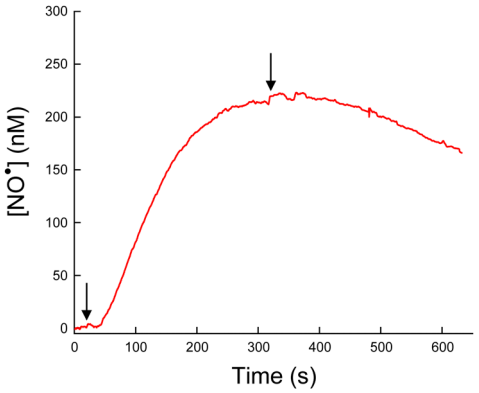

Fig. 9 Chronoamperograms of HC2 under irradiation of 320 s at 400 nm (first arrow: start of irradiation, second arrow: end of irradiation).

room temperature and under irradiation at 400 nm with a lamp of moderate power (order of magnitude of tens of milliwatts). Thermosensitive Ru–NO/PL/CS hydrogels, which were particularly easy to prepare, can therefore be considered as very promising NO-donor materials.

We also investigated the possible impact of the presence of Ru–NO on the viscoelasticity of the gels under irradiation. The gels were thus placed between a transparent lower plate made of glass and an upper stainless steel plate. They were irradiated at 415 nm (20 mW cm^{-2}) for 10 min. No significant effect of the irradiation on the *G′* and *G″* moduli was noted, whatever the nature of the gel, with or without Ru–NO, concentrated or diluted (Fig. S2d, S3d and S6, ESI†).

Because these hydrogels are based only on physical interactions, the dissociation of the hydrogel in contact with a saline buffered solution (PBS) was evaluated. As an early preliminary test before biological experiments, the hydrogel (1.5 mL of HB or HC1, 16.3 wt% PL and 0.8 wt% CS) was placed in contact with PBS at 37 °C for 1 h (exposed top surface: 3.1 cm^2). The excess of the mass of the PBS phase gave the total mass of molecules of the gel released in PBS (all molecules included, *i.e.* chitosan, Pluronics and lactic acid). This mass represented around 40–45 wt% of the total dry mass of the starting gel. This organic matter release was relatively high. It was lower, around 20 wt%, for hydrogels more concentrated in PL and CS (19.4 wt% PL and 1.0 wt% CS; 1.5 mL of the gel; exposed top surface: 3.1 cm^2, also in the gel state at 37 °C). These hydrogels showed similar thermal behaviour and identical morphologies (according to AFM images) as HB. However, their sol–gel transition was about 30 °C, *i.e.* 8 degrees less than the HB hydrogel. In the literature, a 40 wt% release in PBS was also observed but after a period of about 25 h for a PL/CS hydrogel with a composition close to our HB gel (17.5 wt% PL and 0.5 wt% CS, exposed top surface: 4.9 cm^2).[16] Overall, it means that the solubility of these physical hydrogels can be tuned, which makes them interesting as transient or sacrificial materials. The solution above Ru–NO/PL/CS hydrogels was also analysed by UV-vis spectroscopy to evaluate the amount of Ru–NO released, following the absorbance of the characteristic band located at 403 nm of the *trans*-(NO,OH)-[Ru(FT)Cl(NO)(OH)]$^+$

Open Access Article. Published on 05 April 2024. Downloaded on 6/6/2026 6:34:21 AM. This article is licensed under a Creative Commons Attribution-NonCommercial 3.0 Unported Licence.

cation. After 1 h at 37 °C, the amount of Ru–NO in the solution was ~51% of the quantity initially present in the hydrogel (an initial Ru–NO concentration of 1 mM). For GSNO/PL/CS hydrogels[16] (PL and CS compositions identical to ours, an initial GSNO concentration of 50 mM), the amount of GSNO diffused was ~10% after 1 h and ~20% after 4.5 h at 32.5 °C. Nevertheless, the difference in the temperature of the release study, the nature of the NO donor and the large difference in the initial amount made comparison with our results difficult. In two other examples, for PL/CS hydrogels encapsulating respectively dexamethasone[21] or melatonin,[26] releases of ~20% or 40% were observed at 1 hour. Here again, it is almost impossible to compare the analyses, linked to possible differences in chitosan characteristics, in affinities between the hydrogel and the drug molecules.

4. Conclusions

In this study, we have described the first PL/CS-based hydrogels incorporating a water soluble ruthenium nitrosyl complex, namely *trans*-(Cl,Cl)-[Ru(FT)Cl_2(NO)]Cl. Ru–NO/PL/CS hydrogels can be seen as good candidates for nitric oxide release. The NO release under light stimuli was directly evidenced by EPR and by using a NO electrode. Ru–NO/PL/CS hydrogels were easy to prepare and their partial solubility in PBS after a period of 1 h at the physiological temperature made them materials of interest for transient or sacrificial applications. Previous studies have paid attention to $NO^{\bullet}$ as an efficient agent for the treatment of infected wounds because it combines the effect of wound healing processes and broad-spectrum antibacterial activity.[27–30] This work paves the way for future investigation of these hydrogels (whose sol–gel transition can be adjusted by the relative proportions of water and polymers) on wound healing. Work is in progress.

Author contributions

Hazem Gzam: investigation and formal analysis. Dalel Katar: investigation. Marine Tassé: investigation. Yue Xiao: investigation. Isabelle Malfant: conceptualization and writing – review and editing. Juliette Fitremann: investigation, formal analysis, and writing – original draft. Patricia Vicendo: conceptualization. Anne-Françoise Mingotaud: conceptualization and writing – original draft. Dominique de Caro: conceptualization, investigation, and writing – original draft.

Conflicts of interest

There are no conflicts to declare.

Acknowledgements

This work was supported by the Centre National de la Recherche Scientifique (CNRS, France). The authors are grateful for the support from the French National Research Agency under program ANR-20-CE18-0032 (NOBacLight).

References

1 T. R. deBoer and P. K. Mascharak, *Advances in Inorganic Chemistry*, ed. R. van Eldik and J. A. Olabe, Elsevier, Waltham, 2015, vol. 3, pp. 145–170.
2 I. Stepanenko, M. Zalibera, D. Schaniel, J. Telser and V. B. Arion, *Dalton Trans.*, 2022, **51**, 5367.
3 A. J. Gomes, P. A. Barbougli, E. M. Espreafico and E. Tfouni, *J. Inorg. Biochem.*, 2008, **102**, 757.
4 C. Bohlender, M. Wolfram, H. Goerls, W. Imhof, R. Menzel, A. Baumgaertel, U. S. Schubert, U. Mueller, M. Frigge, M. Schnabelrauch, R. Wyrwa and A. Schiller, *J. Mater. Chem.*, 2012, **22**, 8785.
5 J. T. Mitchell-Koch, T. M. Reed and A. S. Borovik, *Angew. Chem., Int. Ed.*, 2004, **43**, 2806.
6 A. C. Roveda Jr., H. de Fanzio Aguiar, K. M. Miranda, C. C. Tadini and D. W. Franco, *J. Mater. Chem. B*, 2014, **2**, 7232.
7 F. Gorzoni Doro, U. P. Rodrigues-Filho and E. Tfouni, *J. Colloid Interface Sci.*, 2007, **307**, 405.
8 E. Tfouni, F. Gorzoni Doro, A. J. Gomes, R. Santana de Silva, G. Metzker, P. G. Zanichelli Benini and D. W. Franco, *Coord. Chem. Rev.*, 2010, **254**, 355.
9 D. C. A. S. de Santana, T. Tallarico Pupo, M. Gama Sauaia, R. Santana da Silva, R. Fonseca and V. Lopez, *Int. J. Pharm.*, 2010, **391**, 21.
10 G. M. Halpenny, M. M. Olmstead and P. K. Mascharak, *Inorg. Chem.*, 2007, **46**, 6601.
11 Y. T. Yu, S. W. Shi, Y. Wang, Q. L. Zhang, S. H. Gao, S. P. Yang and J. G. Liu, *ACS Appl. Mater. Interfaces*, 2020, **12**, 312.
12 J. Akl, I. Sasaki, P. G. Lacroix, I. Malfant, S. Mallet-Ladeira, P. Vicendo, N. Farfán and R. Santillan, *Dalton Trans.*, 2014, **43**, 12721.
13 P. Labra-Vázquez, M. Bocé, M. Tassé, S. Mallet-Ladeira, P. G. Lacroix, N. Farfán and I. Malfant, *Dalton Trans.*, 2020, **49**, 3138. Data for *trans*-(Cl,Cl)-[Ru(FT)Cl_2(NO)]Cl: ^{1}H-NMR δ in ppm: 4.20 (2H, s), 7.44 (2H, m), 7.72 (1H, d), 8.02 (2H, ddd), 8.12 (1H, d), 8.30 (3H, m), 8.55 (2H, td), 9.20 (2H, d), 9.25 (2H, dd), 9.40 (2H, s). FT-IR (ATR, cm^{-1}): 1480 (m, CH_2 scissor), 1620 (s, νC=C), 1690 (m, νC=N), 1880 (s, νNO), 2980–3050 (νCH for sp^3 and sp^2 carbons). UV-vis. λ_{max} in water (ε in M^{-1} cm^{-1}): 286 nm (17 950), 428 nm (9200). MS calculated for $C_{28}H_{19}ON_4Cl_2Ru$: 599.46. Found: 598.92.
14 A. Farhat, M. Tassé, M. Bocé, D. de Caro, I. Malfant, P. Vicendo and A. F. Mingotaud, *Chem. Phys. Lett.*, 2023, **818**, 140434.
15 S. Mika Shishido, A. Barozzi Seabra, W. Loh and M. Ganzarolli de Oliveira, *Biomaterials*, 2003, **24**, 3543.
16 M. T. Pelegrino, B. de Araujo Lima, M. H. M. do Nascimento, C. B. Lombello, M. Brocchi and A. B. Seabra, *Polymers*, 2018, **10**, 452.
17 G. Tavares, P. Alves and P. Simões, *Pharmaceutics*, 2022, **14**, 1377.

 This journal is © The Royal Society of Chemistry and the Centre National de la Recherche Scientifique 2024

Open Access Article. Published on 05 April 2024. Downloaded on 6/6/2026 6:34:21 AM.
This article is licensed under a Creative Commons Attribution-NonCommercial 3.0 Unported Licence.

18 Program Sa3.3 written by D. Lavabre and V. Pimenta. The software can be downloaded at **https://cinet.chim.pagesperso-orange.fr/**.
19 V. Pimenta, C. Frouté, M. H. Deniel, D. Lavabre, R. Guglielmetti and J. C. Micheau, *J. Photochem. Photobiol., A*, 1999, **122**, 199.
20 M. Bocé, M. Tassé, S. Mallet-Ladeira, F. Pillet, C. Da Silva, P. Vicendo, P. G. Lacroix, I. Malfant and M. P. Rols, *Sci. Rep.*, 2019, **9**, 4867.
21 J. García-Couce, M. Tomás, G. Fuentes, I. Que, A. Almirall and L. J. Cruz, *Gels*, 2022, **8**, 44.
22 A. Lupu, L. M. Gradinaru, D. Rusu and M. Bercea, *Gels*, 2023, **9**, 719.
23 J. Akl, I. Sasaki, P. G. Lacroix, V. Hugues, P. Vicendo, M. Bocé, S. Mallet-Ladeira, M. Blanchard-Desce and I. Malfant, *Photochem. Photobiol. Sci.*, 2016, **15**, 1484.
24 O. Schiemann, N. J. Turro and J. K. Barton, *J. Phys. Chem. B*, 2000, **104**, 7214.
25 R. Hübner, B. Sarkar, J. Fiedler, S. Záliš and W. Kaim, *Eur. J. Inorg. Chem.*, 2012, 3569.
26 M. D. Romić, M. S. Klarić, J. Lovrić, I. Pepić, B. Cetina-Čižmek, J. Filipović-Grčić and A. Hafner, *Eur. J. Pharm. Biopharm.*, 2016, **107**, 67.
27 C. G. Kevil, G. K. Kolluru, C. B. Pattillo and T. Giordano, *Free Radic. Biol. Med.*, 2011, **51**, 576.
28 M. B. Witte and A. Barbul, *Am. J. Surg.*, 2002, **183**, 406.
29 O. Ustuner, C. Anlas, T. Bakirel, F. Ustun-Alkan, B. D. Sigirci, S. Ak, H. A. Akpulat, C. Donmez and U. Koca-Caliskan, *Molecules*, 2019, **24**, 3353.
30 J. Lee, S. P. Hlaing, J. Cao, N. Hasan, H. J. Ahn, K. W. Song and J. W. Yoo, *Pharmaceutics*, 2019, **11**, 496.